ELSEVIER

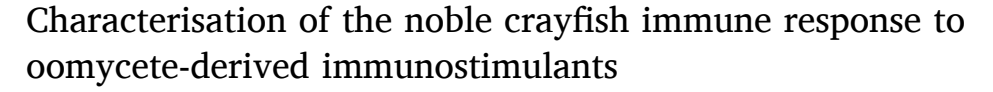
Contents lists available at ScienceDirect

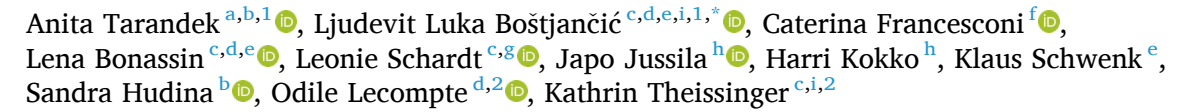
Fish and Shellfish Immunology

journal homepage: www.elsevier.com/locate/fsi



Full length article





- ^a Laboratory of Informatics and Environmental Modelling, Division for Marine and Environmental Research, Ruder Bošković Institute, Bijenička 54, 10000, Zagreb, Croatia
- b Department of Biology, Faculty of Science, University of Zagreb, Horvatovac 102a, 10000, Zagreb, Croatia
- ^c LOEWE Centre for Translational Biodiversity Genomics (LOEWE-TBG), Senckenberganlage 25, 60325, Frankfurt, Germany
- d Department of Computer Science, ICube, UMR 7357, University of Strasbourg, CNRS, Centre de Recherche en Biomédecine de Strasbourg, Rue Eugène Boeckel 1, 67000. Strasbourg, France
- ^e RPTU University Kaiserslautern-Landau, Institute for Environmental Sciences, Fortstraβe7, 76829, Landau, Germany
- f Department of Experimental Medical Science, Lund Stem Cell Center, Lund University, Sölvegatan 19, 221-84, Lund, Sweden
- g Senckenberg Research Institute and Natural History Museum Frankfurt/M, Senckenberganlage 25, 60325, Frankfurt am Main, Germany
- h Department of Environmental and Biological Sciences, University of Eastern Finland, P.O. Box 1627, 70210, Kuopio, Finland
- ⁱ Ecology Department, Faculty of Biology Rhineland-Palatinate University of Technology (RPTU) Kaiserslautern-Landau Erwin-Schrödinger-Str. 14, 67663 Kaiserslautern, Germany

ARTICLE INFO

Keywords: Astacus astacus Aphanomyces astaci Crayfish plague disease Immunostimulation Gene expression Innate immunity Total haemocyte count

ABSTRACT

The invasive oomycete pathogen Aphanomyces astaci significantly threatens native European crayfish populations, prompting investigations towards the effects of protective immunostimulation on the immune response of the vulnerable noble crayfish (Astacus astacus). Here, we evaluate the effect of three oomycete-derived immunostimulant treatments: laminarin (β-1,3-glucan found within the Ap. astaci cell wall), inactivated Ap. astaci spores and Ap. astaci hyphal homogenate. Our findings reveal immediate changes in the noble crayfish total haemocyte count (THC), differential haemocyte count (DHC), and gene expression. A short-term increase in the THC was observed in all treatments, with a gradual return to normal values 8 h post immunostimulation. Granular haemocytes seem to be involved in response to immunostimulation with inactivated Ap. astaci spores, while the number of semi-granular and hyaline haemocytes increased in response to laminarin and Ap. astaci hyphal homogenate. Analysis of the differentially expressed genes showed that the Prophenoloxidase pathway genes and Toll pathway genes are involved in the response to oomycete-derived immunostimulants. Prolonged effects of immunostimulation were reflected in the decreased C/EBP and Kr-h1 gene expression in the hyphal homogenate group as well as decreased Kr-h1 expression in the spore group. Taken together, our results indicate that immunostimulation causes a dynamic change in the noble crayfish immune system response, with similarities in the gene expression patterns between immunostimulated and Ap. astaci infected noble crayfish. As a future research focus, we highlight the importance of molecular characterisation of the genes involved in the anti-oomycete response which could provide valuable insights into pathogen resistance in freshwater crayfish. In the context of the Ap. astaci mediated downfall of the noble crayfish stocks across Europe, further exploration is needed regarding the benefits of the oomycete-derived immunostimulation that can potentially support conservation and aquacultural efforts.

https://doi.org/10.1016/j.fsi.2025.110666

^{*} Corresponding author. Ecology Department, Faculty of Biology Rhineland-Palatinate University of Technology (RPTU) Kaiserslautern-Landau Erwin-Schrödinger-Str. 14, 67663 Kaiserslautern, Germany.

E-mail address: ljudevit-luka.bostanjic@etu.unistra.fr (L.L. Boštjančić).

 $^{^{1}}$ Equally contributing first authors.

² Equally contributing authors.

Abbreviations

AMP – antimicrobial peptide

ALF – anti-lipopolysaccharide factor

ARSH - arylsulfatase H

CBS – crayfish buffered saline

C/EBP - CCAAT-enhancer-binding protein

CPC-1-like - caspase 1-like molecule

DHC - differential haemocyte count

DSCAM – Down syndrome cell adhesion molecule

GNBP - Gram-negative bacteria-binding proteins

Kr-h1 – Krüppel homolog 1

PAMP – pathogen associated molecular pattern
PPAE – prophenoloxidase-activating enzyme
PRR – pathogen recognition receptors

ProPO - prophenoloxidase

PXN – peroxinectin

TEP- Thioester-containing protein

THC – total haemocyte count
TLR – Toll-like receptor

Tollip - Toll-interacting protein

TRAF6 - TNF receptor-associated factor 6

1. Introduction

The invasive oomycete Aphanomyces astaci Schikora (1906), a pathogen of freshwater crayfish originating from North America, is the causative agent of the crayfish plague disease [1]. Since its introduction into Europe with North American freshwater crayfish species, Ap. astaci has decimated native freshwater crayfish populations across the continent [2]. However, co-evolution is re-shaping the interaction between the European host and the pathogen (Jussila et al., 2015; [3]). Recent observations of latently infected European crayfish suggest that some susceptible European crayfish species may have increased their tolerance towards Ap. astaci [4-7]. Early studies already demonstrated that an increased tolerance to Ap. astaci can be induced through immunostimulation with Ap. astaci spores in the susceptible European noble crayfish, Astacus astacus (C. Linnaeus, 1758) [8]. Still, the underlying molecular mechanisms behind this phenomenon remain to date largely unexplored. Understanding how an increased tolerance is achieved through immunostimulation could be pivotal in unveiling the molecular pathways involved in the natural host adaptation.

Freshwater crayfish rely on non-specific innate immunity to defend against pathogens [9,10]. Here, haemocytes represent the primary response mediators in the cellular defence of crayfish against pathogens. Two mechanisms of innate immunity play a prominent role in the cellular defence: phagocytosis of small particles such as microbes and unicellular parasites, and encapsulation of larger parasite invaders [11]. Three types of haemocytes have been identified in freshwater crayfish: hyaline cells, semi-granular cells and granular cells [12]. Granular and semi-granular cells are the predominant types of circulating haemocytes [13]. The hematopoietic tissue is responsible for the production of immature haemocytes (prohemocytes; [14]), and gills are suggested to be a haemocyte reservoir with an important role in maintenance of the haemocyte homeostasis [15]. It is suggested that haemocytes are long-lived cells, developing along a single cell lineage with a maturation period of up to one month from the precursor cells [13]. Pathogen challenges (i.e., interactions with a pathogen that has consequences on the immune status), can influence the total haemocyte count (THC) and differential haemocyte count (DHC), reflecting the changes in the homeostasis [16,17]. During an infection of the noble crayfish with Ap. astaci a significant drop in the THC count has been observed [18,19]. Recognition of the pathogen associated molecular patterns (PAMPs) by

the pathogen recognition receptors (PRRs) leads to the haemocyte degranulation and lysis, requiring active replacement from the hematopoietic tissues or haemocyte reservoirs [15,20].

In addition to the cellular response, the humoral response also plays a role in the innate immune response of the freshwater crayfish to the Ap. astaci infection [21]. The diverse arsenal of humoral response factors is stored in the haemocyte granules or freely circulating in the crayfish haemolymph [22]. Initial studies highlighted the involvement of the prophenoloxidase (proPO) pathway in the response against Ap. astaci, with a constitutively overexpressed proPO in the resistant North American signal crayfish, Pacifastacus leniusculus (Dana, 1852) and lower expression in the susceptible noble crayfish [23]. However, several other humoral factors, such as reactive oxygen species [18], antimicrobial peptides (AMPs) and PRRs likely have a role in the response of freshwater crayfish to Ap. astaci [24]. In particular, the Toll pathway has been connected to the invertebrate anti-fungal response [25,26]. However, in the context of the crayfish immune response towards Ap. astaci the involvement of the Toll pathway has not yet been considered. A better understanding of these humoral responses towards crayfish plague pathogen could be achieved through immunostimulation studies.

Immunostimulation involves exposure to non-lethal pathogen doses, i.e., attenuated forms of the pathogen, closely related non-pathogenic species or molecules that are classified as PAMPs [27,28]. β-1,3-glucan found in the fungal and oomycete cell wall is one of the most well studied PAMPs and a known activator of the proPO pathway [20,29]. In chronically Ap. astaci infected North American signal crayfish, immunostimulation with β-1,3-glucan leads to an increase in granular haemocyte count and increased expression of innate immunity-related proteins (i-type lysozyme, Crustin-like AMP and Masquerade; [30–32]). On the other side, in the susceptible noble crayfish, immunostimulation with β-1,3-glucan leads to an increase in the expression of the transcriptional factor CCAAT/enhancer-binding protein (C/EBP) in the hepatopancreas and the heart of the noble crayfish 4 h post immunostimulation [33]. In addition to C/EBP, the putative transcriptional factor Krüppel homolog-1 (Kr-h1), likely involved in the innate immune response regulation, was also differentially expressed in the noble crayfish challenged with Ap. astaci [24]. Some immunostimulants have successfully been applied as vaccines (i.e. prolonged protection through immunological memory) in invertebrates [34]. However, vaccination approaches towards Ap. astaci have been scarcely investigated, and prolonged effects of different immunostimulants on the noble crayfish have not been explored.

Here, we aimed to characterise the immediate and prolonged changes in the immunological parameters of the noble crayfish following the immunostimulation. To this end, we utilised three different immunostimulants: i) laminarin (β -1,3-glucan found within Ap. astaci cell walls), ii) Ap. astaci hyphal homogenate and iii) inactivated Ap. astaci spores. We analysed changes in circulating haemocytes (by measuring THC and DHC) and immediate (within 1, 4, 8, 24h post injection) and prolonged (within 16-days post injection) changes in the expression of three target genes (proPO, C/EBP and Kr-h1). Additionally, we evaluated the overall gene expression profiles following the immunostimulation through RNA sequencing of the haemolymph. With this approach we wanted to address the following research questions: What is the effect of immunostimulation on the haemocyte homeostasis? Which immune pathways are mediating the response to oomycetederived immunostimulants? Does immunostimulation cause prolonged changes in the monitored parameters? Answering these questions will give us initial indications of whether immunostimulation can induce a prolonged immune protection response in naïve noble crayfish hosts, as well as offer insights into the molecular mechanisms of the anti-oomycete immune response in noble crayfish.

2. Materials and methods

2.1. Experimental animals

A total of 109 (N = 62 in experiment 1 and N = 47 in experiment 2) sexually mature intermoult male noble crayfish were purchased from the crayfish farm Flusskrebszucht Frömel (Kavelstorf, Germany). The average carapace length of the experimental crayfish was 49 mm (SD \pm 4 mm) and the average mass of experimental animals was 23 g (SD \pm 8 g; Supplementary Table 1). Upon arrival, each individual crayfish was placed in a separate aquarium tank filled with 2 L tap water for a 10-day period of acclimatisation. All aquarium tanks were equipped with an aeration pump to ensure a sufficient level of oxygen in the water. The crayfish were monitored and fed daily with one pellet of NovoCrabs (JBL GmbH & Co. Kg, Neuhofen, Germany) and water was exchanged every three days. All experiments involving crayfish were conducted according to the German animal Welfare Act (TierSchG) and Animal Welfare-Experimental Animal Ordinance (TierSchVersV), under the permit number: F 153/Anz,200 issued on the October 21st 2021 with the approval of the Regierungspräsidium Darmstadt.

2.2. Aphanomyces astaci

Strain SATR1 was used for all experiments. The strain was isolated from a signal crayfish in 2012 from Lake Saimaa (Finland), and belongs to the genotype PsI (i.e., haplogroup B based on mitochondrial markers) [35]. The production of *Ap. astaci* zoospores followed the established protocols used in Francesconi et al. [36].

2.3. Preparation of the solutions used for immunostimulation

Crayfish buffered saline (CBS) solution was prepared by dissolving 210~mM NaCl, 5.4~mM KCl, 10~mM CaCl $_2$ x $2H_2O$, 2.4~mM MgCl $_2$ x $6H_2O$ and 2 mM NaHCO₃ in 1 L of water, pH was adjusted to 6.8 with 1 mM KOH [37]. Laminarin solution (5 mg/mL) was prepared by dissolving laminarin (L9634, Sigma-Aldrich, USA) in CBS according to Ekblom et al. [30]. Inactivated Ap. astaci hyphal suspensions were prepared by grinding of blot-dried frozen hyphal tissue in liquid nitrogen and dissolving 0.2 g of the tissue powder in 2 mL of CBS. The suspension was vortexed vigorously and centrifuged at 5000×g for 1 min to remove debris. The clear supernatant was separated from the pellet and aliquoted in 200 μL fractions and stored at $-20~^{\circ}C$ until further use. A final 1:10 dilution of the hyphal supernatant in CBS was used in all experiments. The inactivated Ap. astaci spore solution was prepared according to Ref. [8]. Aliquots of the spore solution containing 2000 spores were placed in separate 1.5 mL microtubes and centrifuged at 10,000×g for 10 min to drop the zoospores into a pellet. The pellet was then resuspended in 100 μ L of CBS and frozen at – 80 °C for 30 min. After 10 min of thawing at room temperature the freezing process was repeated. The solutions were thawed again, vortexed and checked for the presence of the zoospore remains.

2.4. Experimental design

Two separate experiments were conducted to assess immunological parameters of noble crayfish following immunostimulation (Fig. 1). In experiment 1 we investigated immediate changes (1, 4 and 8 h post immunostimulation), while in experiment 2 we investigated prolonged changes (24 h and 16 days post immunostimulation). In both experiments crayfish were assigned to five groups: i) control (untreated), ii) CBS group (injection control), iii) laminarin injection, iv) injection with the homogenate suspension of the inactivated Ap. astaci hyphae, and v) injection with the inactivated Ap. astaci spores. Crayfish were immunostimulated by injecting 100 μL of dedicated solution directly in the hemocoel (dorsally between the cephalothorax and abdomen) using a sterile 26-gauge needle. In experiment 1 (early immune response), 10 control cravfish from the non-injection control group were sampled immediately at the start (0 h) of the experiment, while five crayfish from all four injection groups were sampled at 1 h and 4 h, and three crayfish were sampled at 8 h post immunostimulation. In experiment 2 (prolonged immune response), five crayfish from non-injection control and four crayfish from injection groups were sampled at 24 h, and six crayfish from non-injection control and five crayfish from each of the injection groups were sampled at day 16 post immunostimulation. Finally, we ensured the quality of our results by sampling independent control individuals at critical time points (0, 24 h and 16 days).

2.5. Haemolymph sampling, total and differential haemocyte count

Crayfish haemolymph was sampled from the pericardial sinus using a 26-gauge needle and transferred into cooled 1.5 mL microtube. For the haemocyte counts, 150 μ L of the haemolymph was transferred to a new 1.5 mL microtube which already contained $450 \mu L$ of anticoagulant (1:3 volume). For RNA isolation, 500 µL of the haemolymph was transferred to a new 1.5 mL microtube which already contained 1 mL of anticoagulant (1:2 volume). All samplings were done with precooled equipment and buffers at +4 °C, and samples were kept cool to prevent coagulation. THC was immediately estimated in a Bürker counting chamber under Olympus CX21 LED light microscope (total magnification of 100x) according to Boštjančić et al. [19]. For each sample, haemocytes were counted four times and averaged to estimate the THC per millilitre of haemolymph. For the differential haemocyte count (DHC), at least five micrographs of each replicate from experiment 1 were made at random under Axio Imager M2 phase-contrast microscope equipped with the Axiocam MRc5 microscope camera (total magnification 400x). At least 100 haemocytes per sample were counted to establish the proportion of each haemocyte type (hyaline, granular or semi-granular). The following properties were used to distinguish different haemocyte types according to Ref. [38]: i) hyaline cells - round shape, nucleus to cytoplasm ratio >1, agranular, relative size ~10 μm, ii) semi-granular –

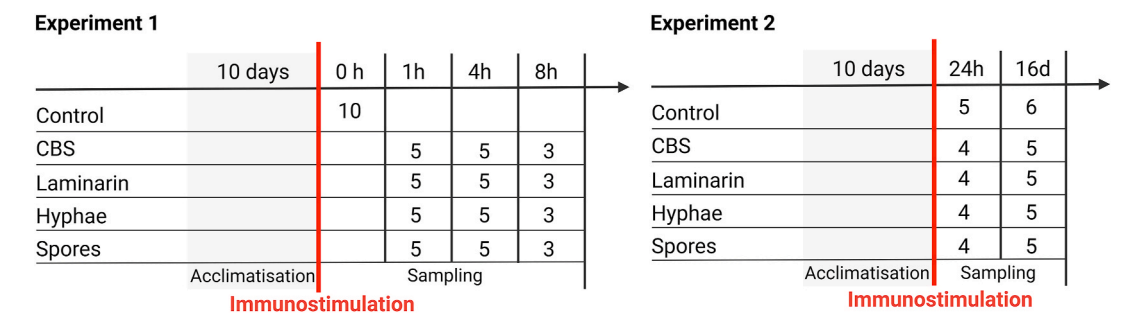


Fig. 1. Experimental design. The number of crayfish for each experiment, experimental group and timepoint is indicated. The experimental groups are the following: control, CBS – injection control with crayfish buffered saline, Laminarin injection, Hyphae – injection with *Ap. astaci* hyphal homogenate, Spores – injection with inactivated *Ap. astaci* spores.

ellipsoid shape, nucleus to cytoplasm ratio \sim 1, variable number of small granules, relative size up to 20 μ m, iii) granular – ellipsoid shape, nucleus to cytoplasm ratio <1, large granules, relative size up to 20 μ m [38] (for reference see Supplementary Fig. 1).

2.6. Analysis of the C/EBP, Kr-h1 and proPO gene expression

Immediately upon sampling, haemolymph was centrifuged at $5000 \times g$ for 5 min at 4 °C. The supernatant was removed, and the cell pellet was washed with 200 μ L CBS to remove EDTA as it inhibits DNases needed in the RNA extraction process. The centrifuging step was repeated and the supernatant removed. The haemolymph cell pellet was stored at - 80 $^{\circ}$ C until RNA isolation. Total RNA from haemolymph cell pellet was isolated using the NuceloSpin RNA Mini kit (Macherey-Nagel, Germany) according to the manufacturers' protocol with the following adjustments: 150 μL Buffer RA1 was used for cell lysis; 150 μL ethanol was used to adjust the RNA binding conditions; 300 µL Buffer RA3 was used for the second wash; instead of the third wash, a drying step was added in which the empty column was centrifuged for 2 min at 11000×g; RNA was eluted two times in the same microtube using 30 μL of RNase-free H₂O each time. RNA quality was assessed on the NanoVue Spectrophotometer, and RNA quantity with the QuantiFluor RNA System on a Quantus fluorometer (Promega, USA). cDNA synthesis was performed using the iScript™ cDNA Synthesis Kit (Bio-Rad, USA) according to the manufacturers' protocol, using half volume reactions and prolonging the reverse transcription step of the protocol to 40 min. Target loci for the qPCR were CCAAT/enhancer-binding protein (C/ EBP), Krüppel homolog-1 (Kr-h1) and prophenoloxidase (proPO), while elongation factor one alpha ($EF1\alpha$) was used as a reference housekeeping gene. Primer pairs C/EBP-F 5'-AGTGGTTGAAAGGCACGACG-3', C/EBP-R 5'-AAACGCCAGCTCCGT.

ACC-3', Kr-h1-F 5'-AGTGTGAGGTGTGCGGTAAG-3', Kr-h1-R 5'-GGCAGTACTC.

ACAGGTGTATGG-3', proPO-F 5'- ACTGGCATCTCGTTTACCCC-3', proPO-R 5'- GTCGTACCTAGCGACCATCTG-3' and EF1 α -F 5'-TGGTGCTTATGAGTTTGTGACAC-3', EF1 α -R 5'-ACATCCTGCAGAGGAAGACG-3' were used as described in Boštjančić et al. [19] and Dobrović et al. [39]. Quantitative polymerase chain reaction (qPCR) was performed using iTaq Universal SYBR Green Supermix (Bio-Rad, USA). qPCR was performed using a CFX Opus 96 Real-Time PCR System (Bio-Rad, USA) according to the manufacturer's specifications. All samples were run in duplicates with the standard deviation of cycle threshold values < 0.5. The difference in the gene expression values between the samples was calculated according to the delta-delta Ct method (2- $\Delta\Delta$ CT) [40].

2.7. RNA sequencing

To better understand the noble crayfish immune response immediately following infection, we conducted RNA sequencing of haemolymph samples obtained from each injection group (in triplicates) 4 h post injection and from non-injection control (in five replicates). This early sampling point was selected for RNA sequencing due to our previously observed changes in the innate immune response parameters in the noble crayfish immunostimulated with laminarin [33]. Library preparation and RNA sequencing (2 x 150 bp paired end reads) was conducted at Novogene Europe (UK), on the Illumina NovaSeq6000. Resulting sequencing quality was checked with FastQC v0.11.9 [41], adapter and quality trimming were conducted using Trimmomatic 0.39 [42] with the ILLUMINACLIP set at 2:30:10, LEADING and TRAILING set to 15, SLIDINGWINDOW set to 4:20 and minimum sequence length set to 50. The results were summarised using MultiQC 1.9 [43]. Accession numbers for raw data and details of the raw and processed reads are available in the Supplementary Table 2.

2.8. Transcriptome assembly, annotation and read mapping

A reference transcriptome was *de novo* assembled using Trinity v2.8.5 with default settings [44]. Assembly quality was assessed using the *TrinityStats.pl* script [44], and transcriptome completeness was assessed using BUSCO 5.3.0, arthropoda_odb10 [45]. Transcriptome functional annotation was conducted according to the Trinotate protocol [46]. Transcript quantification was conducted using *align_and_estimate_abundance.pl* script, with Bowtie set as alignment method and RSEM set as an estimation method [44].

2.9. Differential gene expression analysis

The differential gene expression analysis was conducted according to the DESeq2 protocol [47] implemented in R with the non-injection control set as a reference. Raw counts obtained from the align and estimate_abundance.pl script [44] were used as input. Transcripts originating from the noble crayfish mitogenome (GenBank accession nr.: KX279347.1) were identified using a blastn search [48], with the e-value threshold set to 1e-20. Furthermore, transcripts originating from associated microbiomes (domains: Bacteria and Archaea and kingdom: Fungi) were filtered out based on a DIAMOND 2.0.4 blastx search [49] against the NCBI non-redundant protein database (obtained in March 2022) with the following settings: F 15 -range-culling -top 10 -f 100. Data was then processed with Megan in the -long-read mode, with default settings [50]. Counts for individual Trinity transcript isoforms were grouped to Trinity genes with the tximport R package [51]. Lowly expressed genes were filtered out: only genes with a raw count ≥ 10 across at least three samples (smallest group size) were retained. The package "EnhancedVolcano" [52] was used for the visualisation of the DEGs and "apeglm" for noise removal [53]. The list of DEGs was exported and their counts, log2fold changes and adjusted p-values (FDR = 0.1, p-value = 0.05) together with their respective annotations were merged. Possible overlaps between the DEGs of different treatments were inspected using Venn diagrams implemented in the limma package 3.54.2 [54]. Finally, we identified overlapping DEGs between the dataset of immunostimulated noble crayfish (this study) and noble crayfish under Ap. astaci challenge [24] to identify overlapping genes and pathways.

2.10. Hierarchical clustering and GO enrichment analysis

DEGs were hierarchically clustered with the pheatmap 1.0.12 function in R (CRAN: Package pheatmap (r-project.org)) with the measure of distance set to euclidean and the method to ward.D2. The optimal number of clusters from the resulting DEG dendrogram was evaluated using the sum of squared error metric [55] and silhouettes method [56]. The analysis of the enriched Gene ontology (GO) categories was conducted with topGO 2.50.0 (Bioconductor - topGO), with the weight01 as algorithm, Fisher as test statistic and node size parameter set to 10. The resulting list of enriched GO categories was then summarised with REVIGO 1.8.1 [57], with the species database set to *Drosophila melanogaster* (7227), semantic similarity measure to SimRel and list size to Small (0.5). Resulting relationships between the clusters were visualised in Cytoscape 3.10.2 [58].

2.11. Gene set enrichment analysis

Gene set enrichment analysis was conducted with ClusterProfiler 4.6.2~[59] following the methods described in Boštjančić et al. [24]. Briefly, genes were ranked according to the following transformation: log10(x)/sign(y), where x is the p-value and y log2 fold change. This was followed by enrichment analysis using the "GSEA" function, with the p values adjusted based on Benjamini-Hochberg correction for the multiple hypothesis testing (cutoff <0.05). Graphical representation of the results was obtained using the "gseaplot2" function [59]. The list of

annotated immune related genes is available in the Supplementary Table 3.

2.12. Statistical analysis and data visualisation

All statistical analyses were conducted in R 4.4.1. (R Core Team, 2022). First, the normality of the raw data distribution was tested using the Shapiro-Wilk test. Based on the distribution, it was determined whether parametric (t-test for normal distribution) or non-parametric tests (Wilcoxon rank sum test for non-normal distribution) were used. With these tests, THC, DHC and gene expression data for immunostimulated crayfish were compared to the control group. In all tests a significance level of 5 % was used (p < 0.05). All p-values were adjusted from multiple testing according to the Benjamini-Hochberg adjustment. Data visualisation was conducted within the ggplot2 package (Wickham, 2016). Final editing of results was done in Inkscape 1.1.1 (Ink scape.org).

3. Results

Unless otherwise stated, all results are presented by the measured experimental outcomes in both experiments simultaneously (early and prolonged immune response, respectively). In both experiments, we did not observe mortality associated with immunostimulation.

3.1. Total and differential haemocyte counts

The total haemocyte counts (THC) of the control and the immunostimulated crayfish from *experiment 1* at each time point is presented in Fig. 2A. Overall, immunostimulation induced an increase in THC and shifts in haemocyte composition, with the strongest effects observed within 4 h post injection. Based on the pairwise Wilcoxon rank sum test, a significant increase in THC was recorded: i) at 1 h post immunostimulation in the laminarin group (p-value = 0.0007, V = 0.00) and in the inactivated spore group (p-value = 0.0007, V = 0.00), and ii) at 4 h post

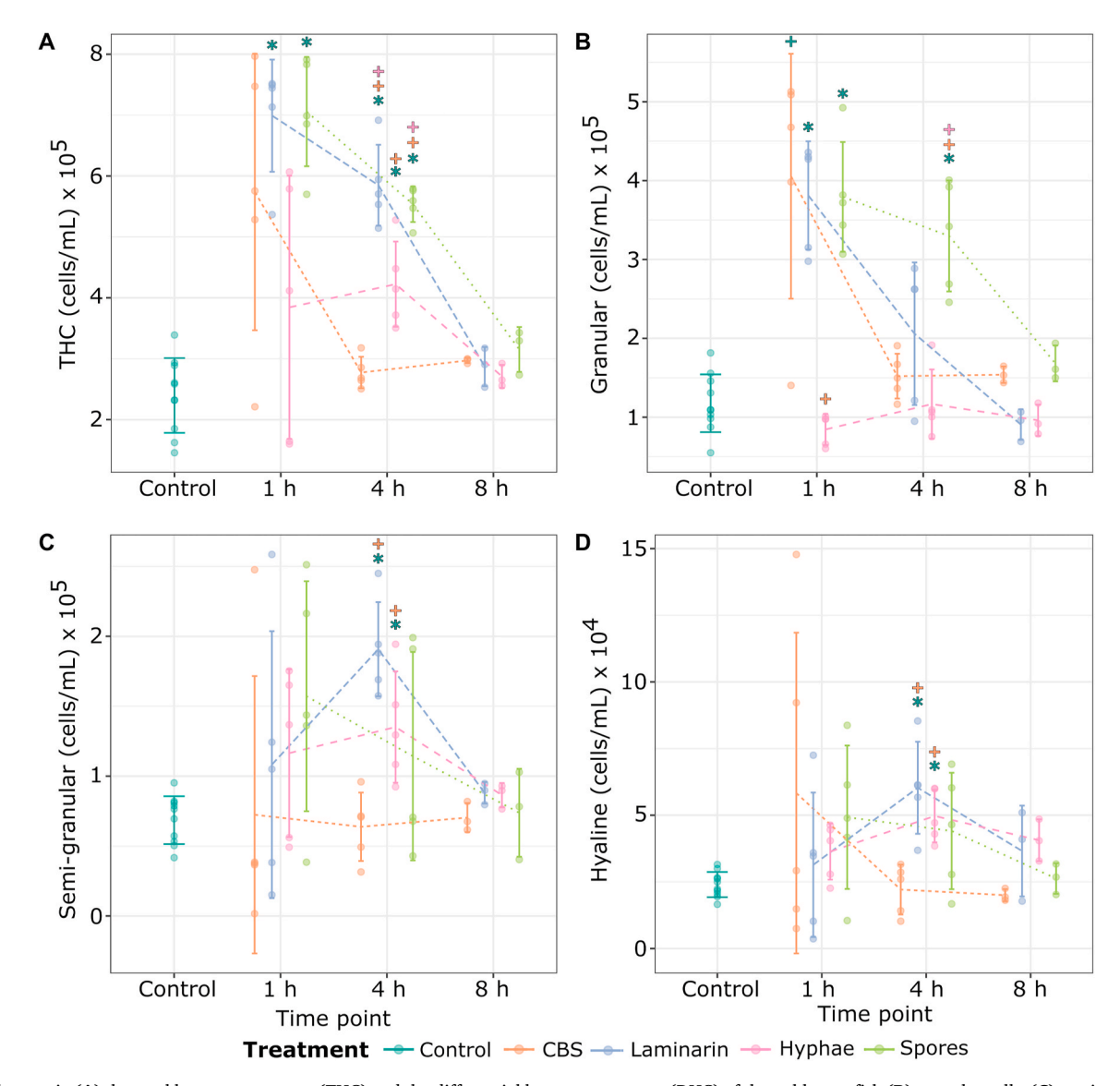


Fig. 2. Changes in (A) the total haemocyte counts (THC) and the differential haemocyte counts (DHC) of the noble crayfish (B) granular cells, (C) semi-granular cells and (D) hyaline cells during immunostimulation in *experiment 1*. Each colour represents a different experimental group: non-injection control (in dark green), crayfish buffered saline (CBS) injected (in orange), laminarin (β -1,3-glucan) injected (in blue), hyphal homogenate injected (in pink), inactivated spore injected (in light green). Four sampling points are marked on the x axis as follows: control, 1h, 4h and 8h post immunostimulation. Timepoints with a statistically significant difference in the haemocyte count from the control are marked in dark green; within each time point statistically significant differences between the groups are marked in the corresponding colours: + (for p-value <0.05) and * (for p-value <0.01). Means of the samples in each group are connected with a line, error bars indicate the standard deviation from the mean.

priming in the laminarin group (p-value = 0.007, V = 0.00), the hyphal homogenate group (p-value = 0.007, V = 0.00) and the inactivated spore group (p-value = 0.007, V = 0.00). No significant changes were observed at 8 h post immunostimulation. In experiment 2, a significant increase in THC was recorded only for the CBS group (injection control; p-value = 0.029, V = 5) at 16 days post immunostimulation (Supplementary Fig. 2). The differential haemocyte counts (DHC) of the control and the immunostimulated noble crayfish in experiment 1 showed a significant increase in the granular haemocytes of the CBS group (p-value = 0.013, V = 3), the laminarin group (p-value = 0.003, V = 0) and the inactivated spore group at 1 h (p-value = 0.003, V = 0) and 4 h (p-value = 0.0007, V = 0) post immunostimulation (Fig. 2B). The number of semi-granular cells was increased in the laminarin group (pvalue = 0.007, V = 1) and in the hyphal homogenate group (p-value = 0.007, V = 0) 4 h post immunostimulation (Fig. 2C), while the number of the hyaline cells was increased in the laminarin group (p-value = 0.003, V = 0) and in the hyphal homogenate group (p-value = 0.003, V = 0) 4 h post immunostimulation (Fig. 2D).

3.2. Expression of C/EBP, Kr-h1 and proPO under immunostimulation

The expression of the selected immune genes C/EBP, Kr-h1 and proPO in haemocytes of control and immunostimulated crayfish at each time point from $experiment\ 1$ and $experiment\ 2$ is presented in Fig. 3. In brief, the expression analysis showed the highest changes in the expression of C/EBP with early up-regulation followed by longer-term down-regulation. The short term up-regulation of proPO was only observed in some treatments. Prolonged down-regulation of Kr-h1 expression was observed in some immunostimulation treatments.

In *experiment 1*, based on the Wilcoxon rank sum test, an upregulation of the C/EBP expression was observed 1 h post immunostimulation in the hyphal homogenate group (p-value = 0.013, V = 1). Four hours post immunostimulation the up-regulation of the C/EBP expression was observed in all four groups: the CBS group (p-value = 0.016, V = 3), the laminarin group (p-value = 0.007, V = 49), the hyphal homogenate group (p-value = 0.007, V = 0), and the inactivated spores group (p-value = 0.032, V = 5). In *experiment 1*, proPO was up-regulated in the CBS group (p-value = 0.035, V = 0) and the inactivated spores group (p-value = 0.035, V = 0). No changes in the expression of Kr-h1 were observed in *experiment 1*.

In *experiment 2*, a down-regulation of the *C/EBP* expression was observed 24 h post-immunostimulation in all four groups: the CBS group (p-value = 0.005, V = 44), the laminarin group (p-value = 0.005, V = 0), the hyphal homogenate group (p-value = 0.044, V = 40), and the inactivated spores group (p-value = 0.005, V = 44). Furthermore, *C/EBP* was still down-regulated 16 days post immunostimulation in the hyphal homogenate group (p-value = 0.005, V = 55). *Kr-h1* was down-regulated in the noble crayfish 16 days post immunostimulation in the hyphal homogenate group (p-value = 0.002, V = 55) and the inactivated spores group (p-value = 0.002, V = 55). There was no change in the expression of *proPO* expression in *experiment 2*.

3.3. Haemolymph transcriptome assembly and annotation

The *de novo* assembled transcriptome of the noble crayfish haemolymph contained 706,985 Trinity transcripts (representative of the 406,935 Trinity genes), with a GC content of 45.22 %, N50 based on all transcript contigs of 593 bp and 95.1 % BUSCO completeness (41.5 % Single copy BUSCOs, 53.6 % duplicated BUSCOs). Detailed statistics of the transcriptome assembly can be found in the Supplementary Table 4. After the assembly filtering based on the expression and contamination, 42,404 trinity genes were retained for downstream analysis. Among the analysed genes, GO assignments based on the functional annotation with the Trinotate pipeline were available for 11,510 (27.14 %) Trinity genes. The assembled transcriptome showed high completeness and quality, providing a robust reference for downstream expression analyses.

3.4. Differentially expressed genes in immunostimulated noble crayfish

Analysis of the differential gene expression showed 54 DEGs in the CBS injection group, 1671 DEGs in the laminarin injection group, 971 DEGs in the hyphal homogenate injection group, and 3723 DEGs in the inactivated spore injection group (Fig. 3A–Supplementary Table 5). DEGs overlapping across all experimental groups were identified as core DEGs, with 13 up-regulated and 6 down-regulated (Supplementary Table 6). Among the core DEGs, eight could be annotated to known protein coding genes including: CCAAT Enhancer Binding Protein (C/EBP), Ras Responsive Element Binding Protein 1-like (RREB1-like), Dual oxidase maturation factor 1-like (DUOXA1-like), ATP Binding Cassette Subfamily A Member 5-like (ABCA5-like), Cytochrome b5-like (CYB5-

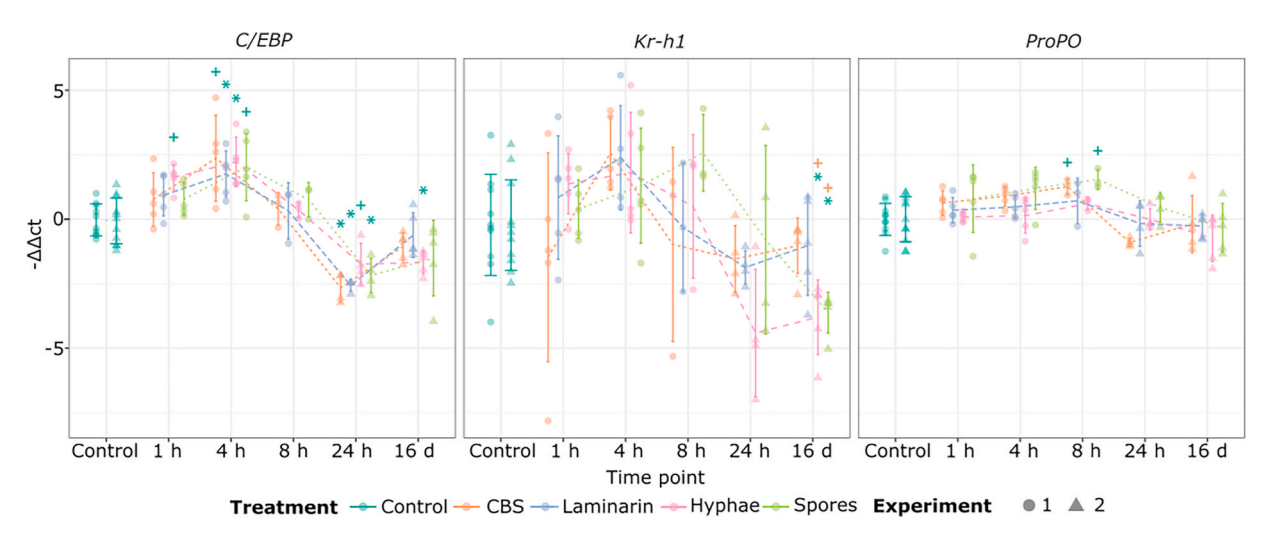


Fig. 3. Analysis of CCAAT/enhancer-binding protein beta (C/EBP), Krüppel homolog 1 (Kr-h1) and prophenoloxidase (proPO) gene expression in the immunostimulated noble crayfish. Each colour represents a different experimental group: non-injection control (in dark green), crayfish buffered saline (CBS) injected (in orange), laminarin (β-1,3-glucan) injected (in blue), hyphal homogenate injected (in pink), inactivated spore injected (in light green). Six sampling points are marked on the x axis as follows: control, 1 h, 4 h, 8 h, 24 h, and 16 d post immunostimulation. Sample replicates from *experiment 1* are marked with circles, while sample replicates from *experiment 2* are marked with triangles. Timepoints with a statistically significant difference in haemocyte count from the control are marked in dark green; within each time point statistically significant differences between the groups are marked in the corresponding colours: + (p-value <0.05) and * (p-value <0.01). Means of the samples in each group are connected with a line, error bars indicate the standard deviation from the mean.

like), Friend leukemia integration 1 transcription factor-like (FLI1-like), Phosphoenolpyruvate carboxykinase (GTP-utilising; PEPCK-G), Tyrosine-protein phosphatase non-receptor type 13-like (PTPN13-like) (Supplementary Tables 5 and 6). Comparative analysis between the DEGs in the immunostimulated and previously identified DEGs in the Ap. astaci infected noble crayfish [24] showed 52 overlapping DEGs (Fig. 4B). Among the overlapping DEGs, ten could be identified as overlapping between all the immunostimulation treatments and eight were annotated to: Kazal-type serine protease inhibitor-like protein, C/EBP, proPO, phenoloxidase-activating factor 2 (PPAE-2), Leukocyte elastase inhibitor (LEI), ETS DNA-binding protein pokkuri-like, Serine/threonine-protein kinase (PIM3), FLI1-like (Supplementary Table 7a). Several other proteins were associated with the prophenoloxidase pathway including phenoloxidase-activating factor 1 (PPAE-1) and peroxinectin (PXN) (Supplementary Table 7). These results highlight that inactivated spores triggered the broadest transcriptional response, including shared immune-related DEGs with infected crayfish, which demonstrates their strong capacity to activate immune responses.

3.5. Gene clusters and gene ontology enrichment

Based on the hierarchical clustering, the existence of two clusters of DEGs was supported (Fig. 5A, Supplementary Fig. 3). The larger cluster 1 (3242 DEGs) contained mostly down-regulated genes, while the smaller cluster 2 (1466 DEGs) contained mostly up-regulated genes in the immunostimulated crayfish (Fig. 5B). Two expression patterns could be observed in cluster 2: a higher expression in the spore treatment of the subcluster 2a and a lower expression in the subcluster 2b (Fig. 5B). GO analysis showed 86 enriched GO terms in the cluster 1 and 204 enriched GO terms in the cluster 2 (p-value <0.05) (Supplementary Table 8). Among the top enriched GO terms in cluster 1 were: membrane fusion, xenobiotic transmembrane transport, positive regulation of DNA-templated DNA replication and cytolysis (Fig. 5C-Supplementary Table 8a). In cluster 2, top enriched GO terms were: innate immune response, T-tubule organisation, multicellular organismal reproductive process and regulation of vascular endothelial growth factor production (Fig. 5C-Supplementary Table 8b). Semantic similarity GO analysis revealed a grouping of the enriched GO terms in cluster 1 into four groups (Supplementary Fig. 4A), while GO terms in cluster 2 were group into one large group (Supplementary Fig. 4B). Cluster-specific GO enrichment suggests differential functional activation of immune and stress response pathways depending on the immunostimulation

treatment.

3.6. Enriched immune gene sets in the immunostimulated noble crayfish

The gene set enrichment analysis of the immunostimulated noble crayfish showed enrichment of the prophenoloxidase (proPO) pathway in all immunostimulation treatments, with the highest enrichment score (0.81) in the hyphae injected noble crayfish, and the lowest enrichment score (0.58) in the CBS injected crayfish (Table 1). Pacifastin-HC/LC was only identified in the spore treated noble crayfish (Table 1). Proteins involved in the immune recognition, antimicrobial peptides and Toll pathway related proteins were enriched in the laminarin and spore immunostimulated noble crayfish (Table 1). Among the core enriched genes in the laminarin treated noble crayfish we identified the PRRs (Gram-negative bacteria-binding proteins (GNBP)), while in the spore treated noble crayfish, we identified the PRRs, Thioester-containing protein (TEP) and mannose-binding lectin (MBL) (Table 1). Together, these findings demonstrate that multiple immune gene sets are differentially activated depending on the immunostimulant, with spores and laminarin treatments inducing the most diverse patterns of immune gene expression.

4. Discussion

Here we characterised the innate immune response of the noble crayfish towards oomycete-derived immunostimulants across multiple time points. Our observations point to an immediate response (up to 4 h) of the innate immune system of the noble crayfish to the immunostimulants, including an increase in THC (Fig. 2A), an altered DHC (Fig. 2B-D), an increase in expression of C/EBP (4 h) followed by decreased C/EBP expression (24 h; Fig. 3) and, based on the RNA sequencing results, an activation of proPO and Toll pathway (4 h; Table 1). We observed an overlap between the DEGs in the immunostimulated crayfish with inactive forms of the pathogen and the DEGs in symptomatic crayfish infected with live Ap. astaci zoospores (Fig. 5). This indicates the activation of similar components of the crayfish immune system when in contact with dead or live Ap. astaci. Moreover, based on the RNAseq analysis we were able to distinguish between changes associated with each immune stimulation treatment (Fig. 5, Table 1). Prolonged changes caused by immunostimulants were observed only in some treatment groups, namely decreased C/EBP and *Kr-h1* expression in the hyphae group and decreased *Kr-h1* expression in the spore group (Fig. 3). In the following, we discuss our findings with

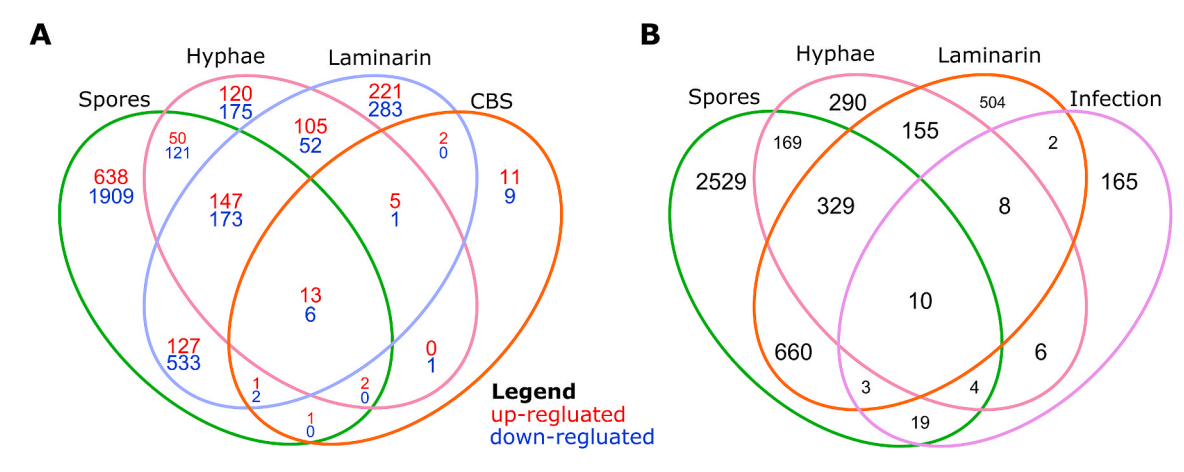


Fig. 4. Results of the differential gene expression analysis in the noble crayfish 4 h post immunostimulation. (A) Venn diagram showing the number of shared differentially expressed genes (DEGs) across all immunostimulation treatments. Up-regulated genes are shown in red and down regulated genes are shown in blue. (B) Venn diagram showing the number of DEGs across all immunostimulation treatments shared with the *Ap. astaci* infected noble crayfish. Identification of the DEGs was conducted within the DESeq2 package [47]. Treatment groups immunostimulation: CBS (injection control), laminarin, hyphal homogenate, inactivated spores. For comparison we utilised the transcriptome of noble crayfish infected with the highly virulent strain of *Ap. astaci* (infection) based on the Boštjančić et al. [24].

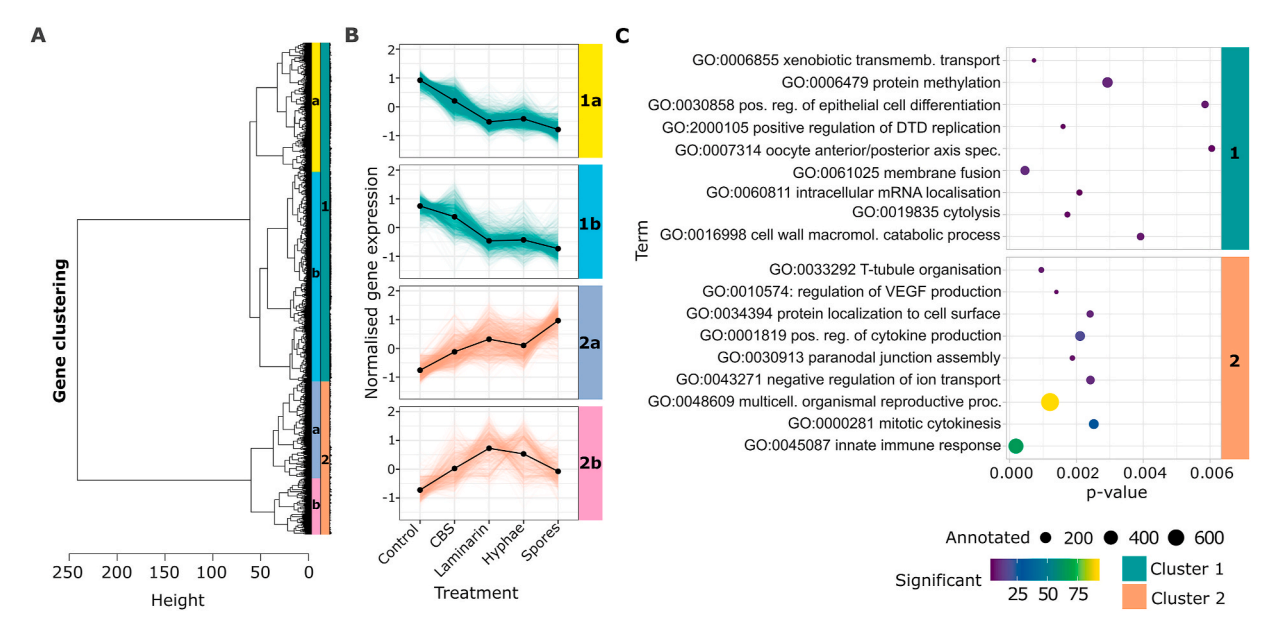


Fig. 5. Results of the hierarchical clustering analysis of the differentially expressed genes (DEGs) across the samples of the immunostimulated noble crayfish. (**A**) Clustering dendrogram showing the assignment of the DEGs into two main clusters (Cluster 1 – green, Cluster 2 – orange), subdivision into subclusters: 1a – yellow, 1b - teal, 2a – blue and 2b – pink. (**B**) Gene expression modules within the clusters, with subdivision based on the expression pattern into subclusters (**C**) Results of the GO enrichment analysis showing top nine enriched GO terms (category: biological process) for clusters 1 and 2.

Table 1

Results of the gene set enrichment analysis for the immunostimulated crayfish. Set size indicates the number of genes in each gene set used for GSEA. *ProPO* - prophenoloxidase, AMP – antimicrobial peptide, *PPAE* – prophenoloxidase-activating enzyme, *PXN* – peroxinectin, CBS (injection control), *C/EBP* – CCAAT-enhancer-binding protein, *Kr-h1* – Krüppel homolog 1, *ARSH* – arylsulfatase H, *CPC-1*-like - caspase 1-like molecule, *GNBP* – Gram-negative bacteria-binding proteins, *DSCAM* – Down syndrome cell adhesion molecule, *ALF* – anti-lipopolysaccharide factor, *Tollip* – Toll-interacting protein, *Tube, TRAF6* – TNF receptor-associated factor 6, *TEP* – Thioester-containing protein, *TLR* – Toll-like receptor, *MBL* – mannose binding lectin.

Treatment	Enriched gene set	Set size	Enrichment score	p-value	p-value (adj.)	Core enriched genes
CBS	ProPO pathway	56	0.58	9.45E- 05	4.72E-04	proPO, PPAE, PXN (2x), C/EBP, Kr-h1, Serpin, Clip SP (4x)
Laminarin	ProPO pathway	56	0.80	5.63E- 13	2.81E-12	ARSH, CPC-1-like, proPO, PPAE (2x), PXN (4x), C/EBP, Kr-h1, Serpin (5x), Clip SP (13x)
	Recognition	43	0.64	1.25E- 04	3.12E-04	GNBP, DSCAM, C-type lectin (4x), Pentraxin, Scavenger A (2x), Scavenger B
	AMPs	12	0.80	3.91E- 03	6.52E-03	Crustin (3x), ALF (3x)
	Toll Pathway	12	0.76	1.02E- 02	1.28E-02	Cactus, Pelle, Dorsal, Tollip, Tube
Hyphae	ProPO pathway	56	0.81	2.55E- 13	1.28E-12	TRAF6, ARSH, proPO, PPAE, PXN (4x), C/EBP, Kr-h1, Serpin (5x), Clip SP (14x)
Spores	ProPO pathway	56	0.77	8.71E- 14	4.35E-13	CPC-1-like, Pacifastin-HC (2x), Pacifastin-LC (1x), ARSH, proPO, PPAE (2x), PXN (4x), C/EBP, Kr-h1, Serpin (3x), Clip SP (9x)
	AMPs	12	0.85	5.16E- 05	1.29E-04	Crustin (2x), ALF (2x)
	Recognition	43	0.54	1.02E- 03	1.70E-03	TEP (4x), MBL, DSCAM, C-type lectin (3x), Pentraxin, Scavenger A (2x), Scavenger B (2x)
	Toll Pathway	12	0.72	9.73E- 03	1.22E-02	TLR, Cactus, Pelle, Dorsal, Tollip, Tube

respect to our three study questions.

4.1. Immunostimulation disrupts haemocyte homeostasis

Throughout our experiments, we did not observe any negative effects of the immunostimulation on noble crayfish survival. Furthermore, as early as 1 h post immune stimulation of the noble crayfish we observed an increase in the THC and a change in the DHC (Fig. 2). The increase in the number of circulating haemocytes likely comes from the release of sessile haemocytes from the gills (haemocyte reservoir), usually rich in the granular haemocyte type [15]. Generally, THC is highly variable among decapod crustaceans [60]. Moreover, changes in THC or DHC of

crustaceans could also reflect changes in the homeostasis of an individual. These could be induced by: hypoxia, moulting period [61], captivity [62], stress caused by transport conditions [63] or environmental contaminants [64]. However, since all stressors were minimized and equal across our experimental groups, we conclude that the observed changes are most likely attributable to alterations in immune status resulting from immunostimulation, as previously reported in Becking et al. [18], Ekblom et al. [30], Boštjančić et al. [19]. Here, we observed an immediate increase (at one and 4 h) in the THC of the β -1, 3-glucan treated noble crayfish, followed by the gradual return to the normal levels within 8 h from the immunostimulation treatment (Fig. 2). Previous immunostimulation studies showed conflicting results of the

THC assessment in the β -1,3-glucan treated freshwater crayfish: an immediate decrease in the THC was reported in signal crayfish [30,31], while reports from the noble crayfish showed both decrease [65] and increase [33] in the THC. Methodological differences in the β -1-3-glucan dose, size of the crayfish individuals and haemolymph sampling approach might explain the differing observations. Moreover, species specific effects of β -1,3-glucan have been reported in other crustaceans and should be considered in the evaluation of the experimental outcomes [66]. Nonetheless, the common observation from all studies is the return to basal levels of THC within 24 h post β -1,3-glucan injection [30, 31]. This return to the basal THC levels was also observed in all experimental groups in this experiment (Fig. 2A).

In our study, noble crayfish injected with the hyphal solution and inactivated spores showed a similar pattern to that of β -1,3-glucan treated noble crayfish, with an increase in the THC at one and 4 h (Fig. 2). This is not surprising, since β -1,3-glucan is a major component of the Ap. astaci cell wall [67] and thus present in the inactivated spores and the hyphal homogenate treatments. At 4 h post immunostimulation, we observed a higher increase in the THC in the laminarin (β -1,3-glucan) and inactivated spore treatment compared to the hyphal extract treatment, suggesting a higher immunostimulation through the injection of the latter (Fig. 2). However, our study was limited by the application of a one single dose concentration of each of the immunostimulants delivered thought the injection. In this context, dosage, number of injections and method of delivery (e.g. injection, immersion or feed) may all influence response magnitude and therefore the immune system response [66]. This challenge should be addressed in future experiments which would investigate the changes in the immune response which are dosage-depended as well as route of administration-dependant. Nevertheless, this result is highly relevant for the interpretation of the gene expression analysis results (sampling point at 4 h), since there are many overlapping DEGs between the spore and laminarin treatments (Fig. 4), as well as a functional overlap in the enriched gene sets (Table 1). In this regard, the results of the DHC are crucial for the interpretation of the DEG analysis.

The DHC showed that an increase in the granular haemocyte count in the laminarin (1 h) and inactivated spore (one and 4 h) treated crayfish (Fig. 2B) is the underlying reason for the change in the THC. A similar pattern of an increase of the number of granular haemocyte was also observed in the laminarin treated signal crayfish [30]. Effects of the β -1, 3-glucan on the granular haemocytes have been studied in vitro in the narrow-clawed crayfish, Pontastacus leptodactylus (Eschscholtz, 1823) where β-1,3-glucan induced a partial degranulation of the granular haemocytes [32], while similar observations were also made in the signal crayfish [68]. Thus, this haemocyte type seems to be particularly important in the response to the immunostimulation with β -1,3-glucan. Finally, in freshwater crayfish haemocyte mobilisation likely occurred from the gills enriched in granular haemocytes [15], thus it is expected to see an increase in granular haemocyte type across all experimental groups. The observed increase in the semi-granular and hyaline haemocytes in the laminarin and hyphae treated crayfish (4 h; Fig. 2C and D) cannot be as easily explained based on the current knowledge of crayfish immunity. However, plausible explanation could be related to their functional role of these haemocyte types in phagocytosis [69] and encapsulation response [32]. On the other hand, the absence of an increase in the number of granular haemocytes in the laminarin and hyphae treatment (4 h) could point to their depletion due to degranulation, or to a return of the sessile granular haemocytes to the tissue of origin [15]. Overall, our results show that immunostimulation causes a short-term disruption in the haemocyte homeostasis both in the haemocyte count and proportion. However, prolonged changes (16 days post injection) in the haemocyte homeostasis were not observed.

4.2. proPO pathway and Toll pathway mediate the response to immunostimulation

Alongside the changes in the haemocyte homeostasis, we observed changes in the gene expression of the immunostimulated noble crayfish (Figs. 3-5). Our results show that the proPO pathway is activated in all immunostimulation treatments including the CBS treatment (Fig. 3, Table 1, Supplementary Table 6). The proPO pathway is a major humoral immune response pathway of freshwater crayfish, characteristic for the semi-granular and granular haemocytes [70]. It is known that the activation of the proPO pathway is stimulated by β -1,3-glucan in the noble crayfish [71]. Multiple immune system reactions are mediated through the proPO pathway: cytotoxic reactions (melanisation), opsonisation, phagocytosis, encapsulation, bacterial clearance and haematopoiesis [72]. Difference in the expression levels and timing of expression of the host proPO enzyme were linked to Ap. astaci resistance in the signal crayfish and susceptibility in the noble crayfish [23]. We also observed that all injected crayfish showed melanisation at the site of injection, which could be a likely explanation for the involvement of the proPO pathway in all treatments, including the injection control with CBS. Indeed, the wound healing and clot hardening processes involve activation of the proPO pathway and deposition of the antimicrobial melanin [73]. This suggests that immediate activation of the proPO pathway is possibly a non-specific response to the method of delivery of the immunostimulants linked to the wound healing reactions.

In this context, we aimed to evaluate the extent to which immunostimulation reflects the actual innate immune response to pathogen challenge. Thus, we compared the DEGs of the immune stimulated crayfish to the DEGs in the crayfish challenged with the highly virulent strain of Ap. astaci (Fig. 4B). The highest overall number of DEGs and the highest number of DEGs shared between the immunostimulated and Ap. astaci infected noble crayfish was observed in the inactivated spore treated noble crayfish (Fig. 4B-Supplementary Table 6). The observed phagocytosis and melanisation of the spores within the haemocytes likely caused a strong immune reaction within the immunostimulated crayfish (Supplementary Fig. 1). These results are also supported by the gene set enrichment analysis, where the proPO pathway, the Toll pathway, recognition proteins and antimicrobial peptides were enriched in the inactivated spore treated and laminarin treated noble crayfish (Table 1). Here, we would again like to stress that a dosage, alongside the type of immunostimulant plays a role in the extant of the immune system activation. This should, however, be further experimentally confirmed, in an experiment where noble crayfish are exposed to different dosage of the immunostimulants.

Among the activated innate immunity pathways, we observed an enrichment of Toll pathway genes in the noble crayfish immunostimulated with spores and laminarin (Table 1). In invertebrates, antibacterial and anti-fungal AMP synthesis is regulated through the Toll pathway [25]. In Drosophila melanogaster, the Toll pathway activation is stimulated by the PGRP receptor recognition of fungal associated β -1, 3-glucan, which leads to the transcription and synthesis of the anti-fungal AMP drosomycin [25]. However, freshwater crayfish lack the PGRP receptors involved in the activation of the Toll pathway, and it has been suggested that the Toll pathway activation is mediated by the Gram-negative binding proteins (GNBP): β-1,3-glucan-binding protein (βGBP) [29], LPS- and β-1,3-glucan-binding protein (LGBP; Supplementary Table 3; [22]). In fact, in D. melanogaster, the Toll pathway can also be activated through another GNBP protein, GNBP3 [26]. GNBPs are enriched in the laminarin treated crayfish, but not in the spore treated crayfish (Table 1). Another explanation for this observation might come from the Chinese mitten crab, Eriocheir sinensis H. Milne-Edwards, 1853, where a possible mechanism of Toll pathway activation could be mediated by Down syndrome cell adhesion molecule (DSCAM) protein [74]. There, cytoplasmic DSCAMs interact with the SH3 domain of the Dock protein which leads to the downstream phosphorylation of the ERK kinase. This kinase, in turn, phosphorylates the

transcription factor Dorsal, enabling the synthesis of AMPs [74]. A similar mode of AMP synthesis involving DSCAM mediated Toll pathway activation might occur in the noble crayfish. Furthermore, the serine proteinase cascade which precedes the cleavage of the cytokine Spätzle (an element of the Toll pathway) and the serine proteinase in the proPO pathway are interconnected [75]. Thus, it is possible that activation of one of the pathways, proPO or Toll, leads to co-activation of the other. An experimental approach including transcriptional silencing of the individual serine proteinase enzymes might reveal a key control protein in this cross-communication.

In addition to the elements of the proPO and Toll pathway, receptors such as DSCAM and C-type lectins are enriched in spore and laminarin treatment (Table 1). Above we described their role in the Toll and proPO pathway activation, but both DSCAM and C-type lectins can also be involved in opsonisation and phagocytosis [76,77]. Moreover, in the spore and laminarin treatment we observed enrichment of scavenger receptors (Table 1). Scavenger receptors are PRRs involved in the phagocytosis, endocytosis, adhesion and signalling [78] and there are

indications of their involvement in the activation of the Toll pathway and AMP synthesis in the mud crab *Scylla paramamosian* Estampador, 1949 [79]. Therefore, given the likely involvement of several differentially expressed receptors in the activation of more than one mechanism of immune response, it seems that the integration of signals from multiple immune pathways is important for the noble crayfish immune response to immunostimulation (Fig. 6). In this context, both the proPO and the Toll pathway and their adjacent elements seem to be likely candidates for future molecular characterisation in the anti-oomycete response of the noble crayfish.

4.3. Prolonged effects of immunostimulation

Apart from short-term effects to the immunostimulants, we also observed prolonged effects (at 16 days) of the immunostimulation regarding a down-regulation of the *C/EBP* gene expression in the hyphal suspension treatment, as well as a down-regulation of the *Kr-h1* gene expression in the hyphal suspension and spore treatments (Fig. 3). We

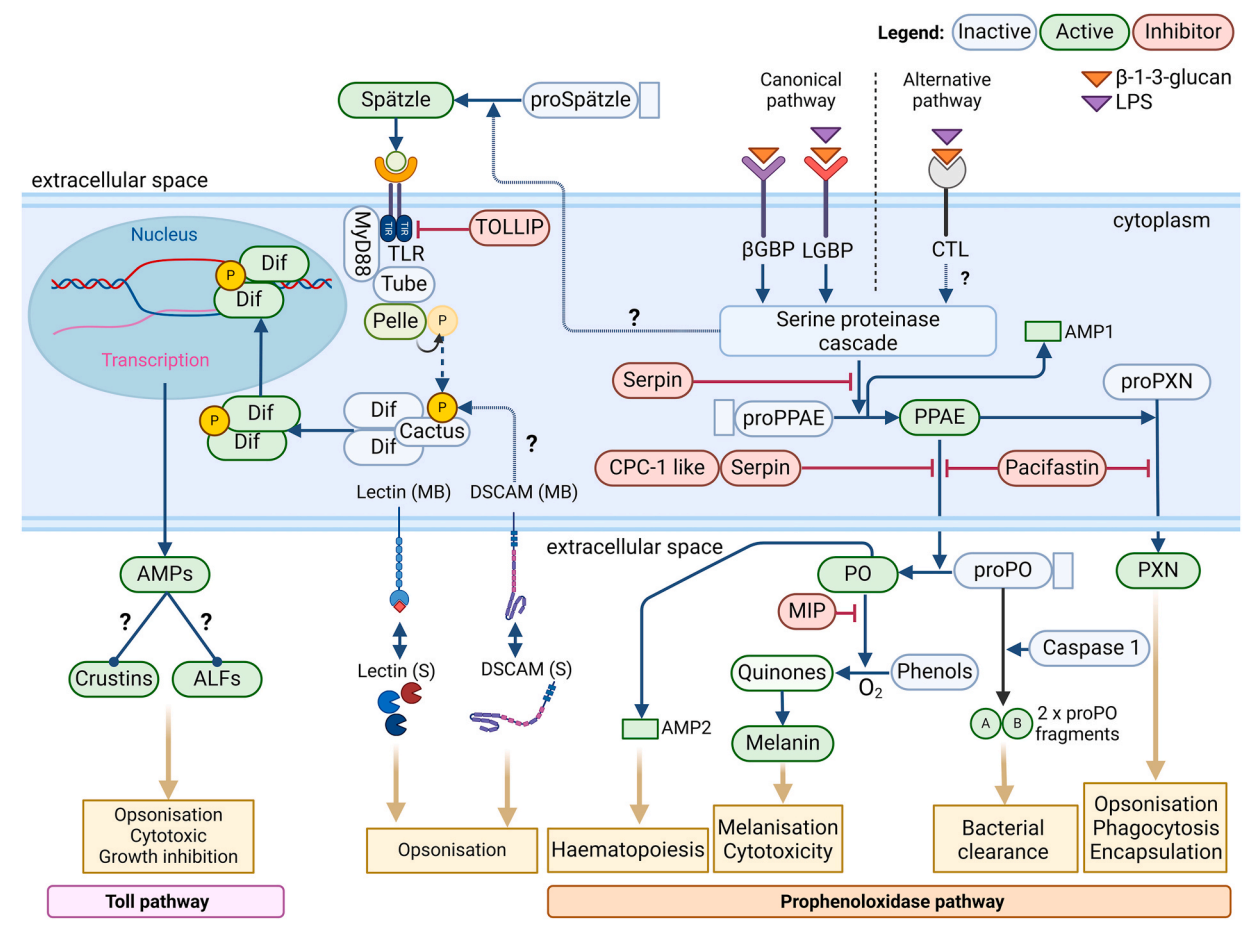


Fig. 6. Schematic representation of the major immune pathways involved in the response to immunostimulation. The prophenoloxidase (proPO) pathway is activated by the pathogen recognition receptors (PRRs) which recognise the β-1,3-glucan present in the hyphal cell wall through β-1,3-glucan-binding protein (βGBP), LPS- and β-1,3-glucan-binding protein (LGBP) or C-type lectin receptor (CTL). This triggers the activation of the serine proteinase cascade that culminates in the activation of the proPO enzyme. The activated phenoloxidase (PO) facilitates the oxidations of monophenols and diphenols to orthoquinones, which then polymerise into the cytotoxic compound melanin. Within the proPO pathway the conversion of the pro-peroxinectin (ProPXN) to peroxinectin (PXN) is triggered. Peroxinectin acts as an opsonin facilitating phagocytosis and encapsulation. The proPO fragments, produced by the Caspase 1 activity, are involved in bacterial clearance, while AMP2 is involved in the haematopoiesis induction. The Toll pathway activation starts with the binding of the cytokine Spätzle by the Toll like receptors (TLRs). This triggers the dimerization of the cytoplasmic TIR domains, which promotes binding of the adaptor protein MyD88, adaptor protein Tube and protein kinase Pelle. This induces the autophosphorylation of Pelle and downstream phosphorylation of the inhibitor Cactus bound to Dorsal-related immunity factor (Dif). Phosphorylated Cactus is degraded while the Dif dimmer transcription factor is translocated to the nucleus, activating the synthesis of the antimicrobial peptides. Pattern recognition receptors (PRRs) such as C-type lectins (CTLs) and Down syndrome cell adhesion molecule (DSCAM) are present either in the membrane bound (MB) or soluble (S) form and involved in the pathogen opsonisation. Alternative activation of proPO pathway can occur through CTLs, while DSCAMs can mediate alternative Toll pathway activation. GNBP - Gram-negative binding proteins, proPPAE - prophenoloxidase activating enzyme, AMP

specifically chose these two molecular target genes as our previous investigations have shown that the transcriptional factors C/EBP and Krh1 are differentially expressed in the noble crayfish under Ap. astaci challenge [19,24]. Moreover, we have provided evidence that at least C/EBP is linked to the innate immune response to laminarin as immunostimulant in the noble crayfish, likely as a transcriptional activator [33]. In the same study, we did not observe a differential expression of Kr-h1 to laminarin [33]. A pattern of C/EBP up-regulation at 4 h, followed by down-regulation observed across all groups at 24 h and persistent down-regulation in the hyphal suspension group after 16 days is indicative of the prolonged effect of immunostimulation on C/EBP expression. On the other hand, the absence of Kr-h1 differential expression at earlier time points and clear down regulation of Kr-h1 expression 16 days post immunostimulation in the hyphae and spore treatments is indicative of delayed response to immunostimulation. Taken together, the results of our gene expression analysis point towards extended changes in gene expression and a need for further investigating and monitoring the innate immune response. Application of RNA sequencing across multiple time points might be beneficial for providing a deeper clarification on the prolonged changes at the gene expression level in the immunostimulated crayfish across broader spectrum of genes.

Finally, in our research we did not observe prolonged changes in the THC of the immunostimulated noble crayfish (Supplementary Fig. 2), while prolonged changes in the DHC are unlikely due to the return of the DHC to normal values 8 h post-immunostimulation. However, potential prolonged changes in the DHC should be analysed in future studies, because in previous invertebrate studies a change in haemocyte number or composition was suggested as an underlying mechanism behind the immune memory response [80]. Previous experiments have shown that immunostimulation with laminarin can induce increased tolerance of the noble crayfish to Ap. astaci [23]. Similarly, multiple sub-lethal immunostimulations with live Ap. astaci spores induced increased resistance to the subsequent Ap. astaci challenge in the noble crayfish [8], suggesting the existence of an innate immune memory in freshwater crayfish. Acquired pathogen resistance or sustained immune response in terms of differential gene expression could be the underlying mechanism behind these observations [80]. However, further experimental evidence is needed to confirm the existence of this phenomenon in freshwater crayfish and its applicability in Ap. astaci disease control.

5. Conclusions

As the native European crayfish populations continue to decline due to Ap. astaci, it is key to assess the potential of innovative conservation methods, such as immunostimulation, to equip the crayfish for survival against the pathogen infection. The innate immune response of the noble crayfish is characterised by a differential expression of multiple innate immune response genes across a number of pathways. Here, we aimed at taking a closer look into the innate immune response towards the treatment with oomycete-derived immunostimulants. Our findings reveal that activation of proPO pathway genes, alongside genes from the Toll pathway, is a characteristic feature of the immune response to oomycete-derived immunostimulant. The changes in the innate immune response towards the immunostimulation were highly dynamic, as reflected in the changes in the THC and DHC and gene expression across the early (1–8 h) time points. Furthermore, based on the gene expression profiles of C/EBP and Kr-h1, immunostimulation could have prolonged effects on the noble crayfish immune status. All three oomycete-derived immunostimulants caused an activation of the immune response. Among them, inactivated spores induced the most extensive transcriptional response, followed by laminarin and hyphal homogenate, indicating treatment-specific variation in immune activation. However, these results should be confirmed in an independent study of the dosage and route of administration studies. Currently, an integrative molecular understanding of the interactions between multiple genes and their innate immune response pathways is lacking. Therefore, we can expect that future studies will use our results to develop these molecular assays. Finally, there is a potential for the oomycete-derived immunostimulants to be applied for conservation or aquaculture purposes if their effects lead to the increased disease tolerance.

Author contributions

Anita Tarandek: Conceptualisation, Data curation, Formal analysis, Investigation, Methodology, Software, Validation, Visualisation, Writing - original draft, Writing – reviewing and editingStructured

Ljudevit Luka Boštjančić: Conceptualisation, Data curation, Formal analysis, Investigation, Methodology, Software, Validation, Visualisation, Supervision, Writing - original draft, Writing - reviewing and editing.

Caterina Francesconi: Conceptualisation, Methodology, Validation, Writing – reviewing and editing.

Lena Bonassin: Investigation, Validation, Writing–reviewing and editing.

Leonie Schardt: Resources, Methodology, Writing – reviewing and editing.

 $\label{lem:conceptualisation} \mbox{ Japo Jussila: Conceptualisation, Validation, Writing} - \mbox{reviewing and editing.}$

 $\label{lem:harrikokko: Conceptualisation, Validation, Writing-reviewing and editing.$

Klaus Schwenk: Supervision, Validation, Writing ${\scriptstyle -}$ reviewing and editing.

Sandra Hudina: Funding acquisition, Project administration, Supervision, Validation, Writing – reviewing and editing.

Odile Lecompte: Conceptualisation, Funding acquisition, Methodology, Formal analysis, Project administration, Resources, Supervision, Validation, Writing – reviewing and editing.

Kathrin Theissinger: Conceptualisation, Funding acquisition, Project administration, Resources, Supervision, Validation, Writing – reviewing and editing.

All authors read and approved the final version of the manuscript.

Declaration of generative AI in scientific writing

During the preparation of this work the author did not use generative AI in scientific writing.

Funding

This study has been funded by the Deutsche Forschungsgemeinschaft (DFG)-Project number 490760095/TH 1807/7-1 and Agence nationale de la recherche Project-ANR-21-CE02-0028. Kathrin Theissinger is supported through the DFG Heisenberg programme (Project number: 534452071/TH 1807/10-1). Ljudevit Luka Boštjančić is supported throught Deutsche Bundesstiftung Umwelt (DBU), Project 39954/01.

Conflict of interest statement

Authors express no conflict of interest.

Acknowledgements

We would like to acknowledge Flusskrebszucht Frömel for the provision of the crayfish for the current study. The authors would like to thank the Department of Environmental and Biological Sciences, University of Eastern Finland, for providing the *Aphanomyces astaci* strain used in this study.

Appendix A. Supplementary data

Supplementary data to this article can be found online at https://doi.

org/10.1016/j.fsi.2025.110666.

Data availability

Data will be made available on request.

References

- D.J. Alderman, J.L. Polglase, Aphanomyces astaci: isolation and culture, J. Fish.
 Dis. 9 (1986) 367–379, https://doi.org/10.1111/j.1365-2761.1986.tb01030.x.
- [2] J. Jussila, L. Edsman, I. Maguire, J. Diéguez-Uribeondo, K. Theissinger, Money kills native ecosystems: european crayfish as an example, Front. Ecol. Evol. 9 (2021), https://doi.org/10.3389/fevo.2021.648495.
- [3] S.V. Hulse, J. Antonovics, M.E. Hood, E.L. Bruns, Host-pathogen coevolution promotes the evolution of general, broad-spectrum resistance and reduces foreign pathogen spillover risk, Evol. Lett. 7 (2023) 467–477, https://doi.org/10.1093/ evlett/grad051.
- [4] M.V. Alvanou, A. Lattos, M.T. Cheimonopoulou, B. Michaelidis, A.P. Apostolidis, I. A. Giantsis, First detection of Aphanomyces astaci and its potential responsibility for mass mortalities of Pontastacus (Astacus) leptodactylus in Greek lakes, J. Biol. Res. 31 (2024) 1–9, https://doi.org/10.26262/jbrt.v31i0.9777.
- [5] J. Jussila, C. Francesconi, K. Theissinger, H. Kokko, J. Makkonen, Is Aphanomyces astaci losing its stamina: a latent crayfish Plague disease agent from Lake Venesjärvi, Finland, Freshw. Crayfish 26 (2021) 139–144, https://doi.org/ 10.5869/fc.2021.v26-2.139.
- [6] J. Jussila, I. Maguire, H. Kokko, V. Tiitinen, J. Makkonen, Narrow-clawed crayfish in Finland: aphanomyces astaci resistance and genetic relationship to other selected European and Asian populations, Knowl. Manag. Aquat. Ecosyst. 2020-Janua 30 (2020), https://doi.org/10.1051/kmae/2020022.
- [7] L. Martín-Torrijos, M. Campos Llach, Q. Pou-Rovira, J. Diéguez-Uribeondo, Resistance to the crayfish plague, Aphanomyces astaci (Oomycota) in the endangered freshwater crayfish species, Austropotamobius pallipes, PLoS One 12 (2017) 1–13, https://doi.org/10.1371/journal.pone.0181226.
- [8] T. Unestam, D.W. Weiss, The host-parasite relationship between freshwater crayfish and the crayfish disease fungus Aphanomyces astaci: responses to infection by a susceptible and a resistant species, J. Gen. Microbiol. 60 (1970) 77–90, https://doi.org/10.1099/00221287-60-1-77.
- [9] L. Cerenius, K. Söderhäll, Crustacean immune responses and their implications for disease control, in: Infectious Disease in Aquaculture, Elsevier, 2012, pp. 69–87, https://doi.org/10.1533/9780857095732.1.69.
- [10] C.F. Low, C.M. Chong, Peculiarities of innate immune memory in crustaceans, Fish Shellfish Immunol. 104 (2020) 605–612, https://doi.org/10.1016/j. fsi.2020.06.047.
- [11] L. Vazquez, J. Alpuche, G. Maldonado, C. Agundis, A. Pereyra-Morales, E. Zenteno, Review: immunity mechanisms in crustaceans, Innate Immun. 15 (2009) 179–188, https://doi.org/10.1177/1753425909102876.
- [12] V.J. Smith, Immunology of invertebrates: cellular, eLS (2016) 1–13, https://doi. org/10.1002/9780470015902.a0002344.pub3.
- [13] F. Li, Z. Zheng, H. Li, R. Fu, L. Xu, F. Yang, Crayfish hemocytes develop along the granular cell lineage, Sci. Rep. 11 (2021) 1–17, https://doi.org/10.1038/s41598-021-02473-9
- [14] I. Söderhäll, E. Bangyeekhun, S. Mayo, K. Söderhäll, Hemocyte production and maturation in an invertebrate animal; proliferation and gene expression in hematopoietic stem cells of Pacifastacus leniusculus, Dev. Comp. Immunol. 27 (2003) 661–672, https://doi.org/10.1016/S0145-305X(03)00039-9.
- [15] Z. Zheng, F. Li, H. Li, K. Zhu, L. Xu, F. Yang, Rapid regulation of hemocyte homeostasis in crayfish and its manipulation by viral infection, Fish Shellfish Immunol. Reports 2 (2021) 100035, https://doi.org/10.1016/j. fsirep.2021.100035.
- [16] S. Dutta, B. Biswas, B. Guha, Sex specific quantitative estimation of total haemocytes in mud crab, Scylla serrata (Forskal, 1775): an evidenced based report, J. Entomol. Zool. Stud. 9 (2021) 439–441, https://doi.org/10.22271/j.ento.2021. v9.i4f.8814.
- [17] M.W. Johansson, P. Keyser, K. Sritunyalucksana, K. Söderhäll, Crustacean haemocytes and haematopoiesis, Aquaculture 191 (2000) 45–52, https://doi.org/ 10.1016/S0044-8486(00)00418-X.
- [18] T. Becking, A. Mrugala, C. Delaunay, J. Svoboda, M. Raimond, S. Viljamaa-Dirks, A. Petrusek, F. Grandjean, C. Braquart-Varnier, Effect of experimental exposure to differently virulent Aphanomyces astaci strains on the immune response of the noble crayfish Astacus astacus, J. Invertebr. Pathol. 132 (2015) 115–124, https:// doi.org/10.1016/j.jip.2015.08.007.
- [19] L.L. Boštjančić, C. Francesconi, L. Bonassin, S. Hudina, R. Gračan, I. Maguire, C. Rutz, A. Beck, A. Dobrović, O. Lecompte, K. Theissinger, Temporal dynamics of the immune response in Astacus astacus (Linnaeus, 1758) challenged with Aphanomyces astaci Schikora, 1906, Fish Shellfish Immunol. 143 (2023) 109185, https://doi.org/10.1016/j.fsi.2023.109185.
- [20] L. Cerenius, K. Söderhäll, Arthropoda: pattern recognition proteins in Crustacean immunity, in: Advances in Comparative Immunology, Springer International Publishing, Cham, 2018, pp. 213–224, https://doi.org/10.1007/978-3-319-76768-0_10.
- [21] Y. Bouallegui, A comprehensive review on crustaceans' immune System with a focus on freshwater crayfish in relation to crayfish plague disease, Front. Immunol. 12 (2021) 1–15, https://doi.org/10.3389/fimmu.2021.667787.

- [22] L. Cerenius, K. Söderhäll, Crayfish immunity recent findings, Dev. Comp. Immunol. 80 (2018) 94–98, https://doi.org/10.1016/j.dci.2017.05.010.
- [23] L. Cerenius, E. Bangyeekhun, P. Keyser, I. Söderhäll, K. Söderhäll, Host prophenoloxidase expression in freshwater crayfish is linked to increased resistance to the crayfish plague fungus, Aphanomyces astaci, Cell. Microbiol. 5 (2003) 353–357, https://doi.org/10.1046/j.1462-5822.2003.00282.x.
- [24] L.L. Boštjančić, C. Francesconi, C. Rutz, L. Hoffbeck, L. Poidevin, A. Kress, J. Jussila, J. Makkonen, B. Feldmeyer, M. Bálint, K. Schwenk, O. Lecompte, K. Theissinger, Host-pathogen coevolution drives innate immune response to Aphanomyces astaci infection in freshwater crayfish: transcriptomic evidence, BMC Genom. 23 (2022) 600, https://doi.org/10.1186/s12864-022-08571-z.
- [25] B. Lemaitre, E. Nicolas, L. Michaut, J.M. Reichhart, J.A. Hoffmann, The dorsoventral regulatory gene cassette spatzle/Toll/Cactus controls the potent antifungal response in Drosophila adults, Cell 86 (1996) 973–983, https://doi.org/ 10.1016/S0092-8674(00)80172-5.
- [26] S.A. Lindsay, S.A. Wasserman, Conventional and non-conventional Drosophila Toll signaling, Dev. Comp. Immunol. 42 (2014) 16–24, https://doi.org/10.1016/j. dci.2013.04.011.
- [27] Y.H. Chang, R. Kumar, T.H. Ng, H.C. Wang, What vaccination studies tell us about immunological memory within the innate immune system of cultured shrimp and crayfish, Dev. Comp. Immunol. (2018), https://doi.org/10.1016/j. dci.2017.03.003. Elsevier Ltd.
- [28] V.J. Smith, J.H. Brown, C. Hauton, Immunostimulation in crustaceans: does it really protect against infection? Fish Shellfish Immunol. 15 (2003) 71–90, https://doi.org/10.1016/S1050-4648(02)00140-7.
- [29] K. Söderhäll, Fungal cell wall β-1,3-glucans induce clotting and phenoloxidase attachment to foreign surfaces of crayfish hemocyte lysate, Dev. Comp. Immunol. 5 (1981) 565–573, https://doi.org/10.1016/s0145-305x(81)80031-6.
- [30] C. Ekblom, K. Söderhäll, I. Söderhäll, Early changes in crayfish hemocyte proteins after injection with a β-1,3-glucan, compared to saline injected and naive animals, Int. J. Mol. Sci. 22 (2021) 1–20, https://doi.org/10.3390/ijms22126464.
- [31] M. Persson, L. Cerenius, K. Soderhall, The influence of haemocyte number on the resistance of the freshwater crayfish, Pacifastacus leniusculus Dana, to the parasitic fungus Aphanomyces astaci, J. Fish. Dis. 10 (1987) 471–477, https://doi.org/ 10.1111/j.1365-2761.1987.tb01098.x.
- [32] M. Persson, A. Vey, K. Söderhäll, Encapsulation of foreign particles in vitro by separated blood cells from crayfish, Astacus leptodactylus, Cell Tissue Res. 247 (1987) 409–415, https://doi.org/10.1007/BF00218322.
- [33] L. Bostjančić, P. Dragičević, L. Bonassin, C. Francesconi, A. Tarandek, L. Schardt, C. Rutz, S. Hudina, K. Schwenk, O. Lecompte, K. Theissinger, Expression of C/EBP and Kr-h1 transcription factors under immune stimulation in the noble crayfish, Gene 929 (2024), https://doi.org/10.1016/j.gene.2024.148813.
- [34] J. Contreras-Garduño, H. Lanz-Mendoza, B. Franco, A. Nava, M. Pedraza-Reyes,
 J. Canales-Lazcano, Insect immune priming: ecology and experimental evidences,
 Ecol. Entomol. 41 (2016) 351–366, https://doi.org/10.1111/een.12300.
 [35] J. Makkonen, J. Jussila, J. Panteleit, N.S. Keller, A. Schrimpf, K. Theissinger,
- [35] J. Makkonen, J. Jussila, J. Panteleit, N.S. Keller, A. Schrimpf, K. Theissinger, R. Kortet, L. Martín-Torrijos, J.V. Sandoval-Sierra, J. Diéguez-Uribeondo, H. Kokko, Jenny, J. Jussila, J. Panteleit, N.S. Keller, A. Schrimpf, K. Theissinger, R. Kortet, L. Martín-Torrijos, J.V. Sandoval-Sierra, J. Diéguez-Uribeondo, H. Kokko, MtDNA allows the sensitive detection and haplotyping of the crayfish plague disease agent Aphanomyces astaci showing clues about its origin and migration, Parasitology 145 (2018) 1210–1218, https://doi.org/10.1017/S0031182018000227.
- [36] C. Francesconi, J. Makkonen, A. Schrimpf, J. Jussila, H. Kokko, K. Theissinger, Controlled infection experiment with Aphanomyces astaci provides additional evidence for latent infections and resistance in freshwater crayfish, Front. Ecol. Evol. (2021), https://doi.org/10.3389/fevo.2021.647037.
- [37] A. Goldina, T.M. Simms, T. Pitzer, S.W. Street, M. Fl, Once a Loser always a Loser? Using crayfish to teach behavioral endocrinology, Test. Stud. Lab. TeachingProceedings Assoc. Biol. Lab. Educ. 32 (2011) 354–359.
- [38] A.F. Rowley, The Immune System of Crustaceans, Encyclopedia of Immunobiology, Elsevier, 2016, https://doi.org/10.1016/B978-0-12-374279-7.12005-3.
- [39] A. Dobrović, S. Geček, T. Klanjšček, I. Haberle, P. Dragičević, D. Pavić, A. Petelinec, L.L. Boštjančić, L. Bonassin, K. Theissinger, S. Hudina, Recurring infection by crayfish plague pathogen only marginally affects survival and growth of marbled crayfish, NeoBiota 77 (2022) 155–177, https://doi.org/10.3897/ neobiota.77.87474.
- [40] K.J. Livak, T.D. Schmittgen, Analysis of relative gene expression data using real-time quantitative PCR and the $2-\Delta\Delta$ CT method, Methods 25 (2001) 402–408, https://doi.org/10.1006/meth.2001.1262.
- [41] S. Andrews, FastQC: a quality control tool for high throughput sequence data, Available at: http://www.bioinformatics.babraham.ac.uk/projects/fastqc/, 2010.
- [42] A.M. Bolger, M. Lohse, B. Usadel, Trimmomatic: a flexible trimmer for Illumina sequence data, Bioinformatics 30 (2014) 2114–2120, https://doi.org/10.1093/ bioinformatics/btu170.
- [43] P. Ewels, M. Magnusson, S. Lundin, M. Käller, MultiQC: summarize analysis results for multiple tools and samples in a single report, Bioinformatics 32 (2016) 3047–3048, https://doi.org/10.1093/bioinformatics/btw354.
- [44] M.G. Grabherr, Brian J. Haas, Moran Yassour Joshua Z. Levin, Dawn A. Thompson, Ido Amit, Xian Adiconis, Lin Fan, Raktima Raychowdhury, Qiandong Zeng, Zehua Chen, Evan Mauceli, Hacohen Nir, Andreas Gnirke, Nicholas Rhind, di Palma Federica, W.N. Bruce, Friedman, A.R, Trinity: reconstructing a full-length transcriptome without a genome from RNA-Seq data, Nat. Biotechnol. 29 (2013) 644–652, https://doi.org/10.1038/nbt.1883.Trinity.

- [45] M. Seppey, M. Manni, E.M. Zdobnov, BUSCO: Assessing Genome Assembly and Annotation Completeness, His Master's Voice, 2019, pp. 227–245, https://doi.org/ 10.1007/978-1-4939-9173-0_14.
- [46] D.M. Bryant, K. Johnson, T. DiTommaso, T. Tickle, M.B. Couger, D. Payzin-Dogru, T.J. Lee, N.D. Leigh, T. Kuo, F.G. Davis, J. Bateman, S. Bryant, A.R. Guzikowski, S. L. Tsai, S. Coyne, W.W. Ye, R.M. Freeman, L. Peshkin, C.J. Tabin, A. Regev, B. J. Haas, J.L. Whited, A Tissue-Mapped Axolotl De Novo Transcriptome Enables Identification of Limb Regeneration Factors, Cell Rep. 18 (2017) 762–776, https://doi.org/10.1016/j.celrep.2016.12.063.
- [47] M.I. Love, W. Huber, S. Anders, Moderated estimation of fold change and dispersion for RNA-seq data with DESeq2, Genome Biol. 15 (2014) 550, https:// doi.org/10.1186/s13059-014-0550-8.
- [48] C. Camacho, G. Coulouris, V. Avagyan, N. Ma, J. Papadopoulos, K. Bealer, T. L. Madden, BLAST+: architecture and applications, BMC Bioinf. 10 (2009) 421, https://doi.org/10.1186/1471-2105-10-421.
- [49] B. Buchfink, C. Xie, D.H. Huson, Fast and sensitive protein alignment using DIAMOND, Nat. Methods 12 (2015) 59–60, https://doi.org/10.1038/nmeth.3176.
- [50] C. Bağcı, S. Patz, D.H. Huson, DIAMOND+MEGAN: fast and easy taxonomic and functional analysis of short and long microbiome sequences, Curr. Protoc. 1 (2021) 1–30, https://doi.org/10.1002/cpz1.59.
- [51] C. Soneson, M.I. Love, M.D. Robinson, Differential analyses for RNA-seq: transcript-level estimates improve gene-level inferences, F1000Research 4 (2015) 1521, https://doi.org/10.12688/f1000research.7563.1.
- [52] K. Blighe, S. Rana, M. Lewis, EnhancedVolcano: publication-Ready volcano plots with enhanced colouring and labeling, Available at: https://github.com/kevinblighe/EnhancedVolcano, 2020.
- [53] A. Zhu, J.G. Ibrahim, M.I. Love, Heavy-tailed prior distributions for sequence count data: removing the noise and preserving large differences, Bioinformatics 35 (2019) 2084–2092, https://doi.org/10.1093/bioinformatics/bty895.
- [54] M.E. Ritchie, B. Phipson, D. Wu, Y. Hu, C.W. Law, W. Shi, G.K. Smyth, Limma powers differential expression analyses for RNA-Sequencing and microarray studies, Nucleic Acids Res. 43 (2015), https://doi.org/10.1093/nar/gkv007 e47.e47
- [55] T. Thinsungnoen, N. Kaoungku, P. Durongdumronchai, K. Kerdprasop, N. Kerdprasop, The clustering validity with silhouette and sum of squared errors, 44–51, https://doi.org/10.12792/iciae2015.012, 2015.
- [56] P.J. Rousseeuw, Silhouettes: a graphical aid to the interpretation and validation of cluster analysis, J. Comput. Appl. Math. 20 (1987) 53–65, https://doi.org/ 10.1016/0377-0427(87)90125-7.
- [57] F. Supek, M. Bošnjak, N. Škunca, T. Šmuc, Revigo summarizes and visualizes long lists of gene ontology terms, PLoS One 6 (2011), https://doi.org/10.1371/journal. pone.0021800.
- [58] P. Shannon, A. Markiel, O. Ozier, N.S. Baliga, J.T. Wang, D. Ramage, N. Amin, B. Schwikowski, T. Ideker, Cytoscape: a software environment for integrated models of biomolecular interaction networks, Genome Res. 13 (2003) 2498–2504, https://doi.org/10.1101/gr.1239303.
- [59] G. Yu, L.-G. Wang, Y. Han, Q.-Y. He, clusterProfiler: an R package for comparing biological themes among gene clusters, OMICS A J. Integr. Biol. 16 (2012) 284–287, https://doi.org/10.1089/omi.2011.0118.
- [60] Y. Su, F. Yang, F. Li, Comparison analysis of circulating hemocytes in decapod crustaceans, Fish Shellfish Immunol. 154 (2024) 109947, https://doi.org/ 10.1016/i.fsi.2024.109947.
- [61] T. Sequeira, D. Tavares, M. Arala-Chaves, Evidence for circulating hemocyte proliferation in the shrimp Penaeus japonicus, Dev. Comp. Immunol. 20 (1996) 97–104, https://doi.org/10.1016/0145-305X(96)00001-8.
- [62] S. Taylor, M.J. Landman, N. Ling, Flow cytometric characterization of freshwater crayfish hemocytes for the examination of physiological status in wild and captive

- animals, J. Aquat. Anim. Health 21 (1) (2009) 195–203, https://doi.org/10.1577/H09-003.
- [63] J. Jussila, M. Paganini, S. Mansfield, L.H. Evans, On physiological responses, plasma glucose, total hemocyte counts and dehydration, of marron Cherax tenuimanus (Smith) to Handling and transportation under simulated conditions, Freshw. Crayfish 12 (1999) 154–167.
- [64] G. Le Moullac, P. Haffner, Environmental factors affecting immune responses in Crustacea, Aquaculture 191 (2000) 121–131, https://doi.org/10.1016/S0044-8486(00)00422-1.
- [65] V.J. Smith, K. Söderhäll, β -l, 3 Glucan activation of Crustacean hemocytes in vitro and in vivo, Biol. Bull. 164 (1983) 299–314, https://doi.org/10.2307/1541146.
- [66] K. Mohan, S. Ravichandran, T. Muralisankar, V. Uthayakumar, R. Chandirasekar, P. Seedevi, R.G. Abirami, D.K. Rajan, Application of marine-derived polysaccharides as immunostimulants in aquaculture: a review of current knowledge and further perspectives, Fish Shellfish Immunol. 86 (2019) 1177–1193, https://doi.org/10.1016/j.fsi.2018.12.072.
- [67] L. Nyhlén, T. Unestam, Cyst and germ tube wall structure in Aphanomyces astaci, Oomycetes, Can. J. Microbiol. 24 (1978) 1296–1299, https://doi.org/10.1139/ m78-210.
- [68] M.A. Barracco, B. Duvic, K. Söderhäll, The β-1,3-glucan-binding protein from the crayfish Pacifastacus leniusculus, when reacted with a β-1,3-glucan, induces spreading and degranulation of crayfish granular cells, Cell Tissue Res. 266 (1991) 491–497, https://doi.org/10.1007/BF00318590.
- [69] M.W. Johansson, K. Soderhall, Cellular immunity in crustaceans and the proPO system, Parasitol. Today 5 (1989) 171–176, https://doi.org/10.1016/0169-4758 (80)90139-7
- [70] L. Cerenius, B.L. Lee, K. Söderhäll, The proPO-system: pros and cons for its role in invertebrate immunity, Trends Immunol. 29 (2008) 263–271, https://doi.org/ 10.1016/j.it.2008.02.009.
- [71] T. Unestam, K. Söderhäll, Soluble fragments from fungal cell walls elicit defence reactions in crayfish, Nature 267 (1977) 45–46, https://doi.org/10.1038/ 267045a0.
- [72] L. Cerenius, K. Söderhäll, Immune properties of invertebrate phenoloxidases, Dev. Comp. Immunol. 122 (2021), https://doi.org/10.1016/j.dci.2021.104098.
- [73] U. Theopold, O. Schmidt, K. Söderhäll, M.S. Dushay, Coagulation in arthropods: defence, wound closure and healing, Trends Immunol. 25 (2004) 289–294, https://doi.org/10.1016/j.it.2004.03.004.
- [74] D. Li, Z. Wan, X. Li, M. Duan, L. Yang, Z. Ruan, Q. Wang, W. Li, Alternatively spliced Down syndrome cell adhesion molecule (Dscam) controls innate immunity in crab, J. Biol. Chem. 294 (2019) 16440–16450, https://doi.org/10.1074/jbc. PA-110.010347.
- [75] L. Cerenius, S. Kawabata, B.L. Lee, M. Nonaka, K. Söderhäll, Proteolytic cascades and their involvement in invertebrate immunity, Trends Biochem. Sci. 35 (2010) 575–583, https://doi.org/10.1016/j.tibs.2010.04.006.
- [76] X.W. Wang, G.R. Vasta, J.X. Wang, The functional relevance of shrimp C-type lectins in host-pathogen interactions, Dev. Comp. Immunol. 109 (2020) 103708, https://doi.org/10.1016/j.dci.2020.103708.
- [77] A. Watthanasurorot, P. Jiravanichpaisal, H. Liu, I. Söderhäll, K. Söderhäll, Bacteria-induced Dscam isoforms of the crustacean, Pacifastacus leniusculus, PLoS Pathog. 7 (2011), https://doi.org/10.1371/journal.ppat.1002062.
- [78] A. Alquraini, J. El Khoury, Scavenger receptors, Curr. Biol. 30 (2020) R790–R795, https://doi.org/10.1016/j.cub.2020.05.051
- [79] N.T. Tran, H. Liang, M. Zhang, M.A.H. Bakky, Y. Zhang, S. Li, Role of cellular receptors in the innate immune System of crustaceans in response to white spot syndrome virus, Viruses 14 (2022) 1–18, https://doi.org/10.3390/v14040743.
- [80] D. Melillo, R. Marino, P. Italiani, D. Boraschi, Innate immune memory in invertebrate metazoans: a critical appraisal, Front. Immunol. 9 (2018) 1915, https://doi.org/10.3389/fimmu.2018.01915.